Supplement of Biogeosciences, 14, 3157–3169, 2017
https://doi.org/10.5194/bg-14-3157-2017-supplement

Biogeosciences
Open Access

Supplement of

Spatial variability of CO_2 uptake in polygonal tundra: assessing low-frequency disturbances in eddy covariance flux estimates

Norbert Pirk et al.

Correspondence to: Norbert Pirk (norbert.pirk@nateko.lu.se)

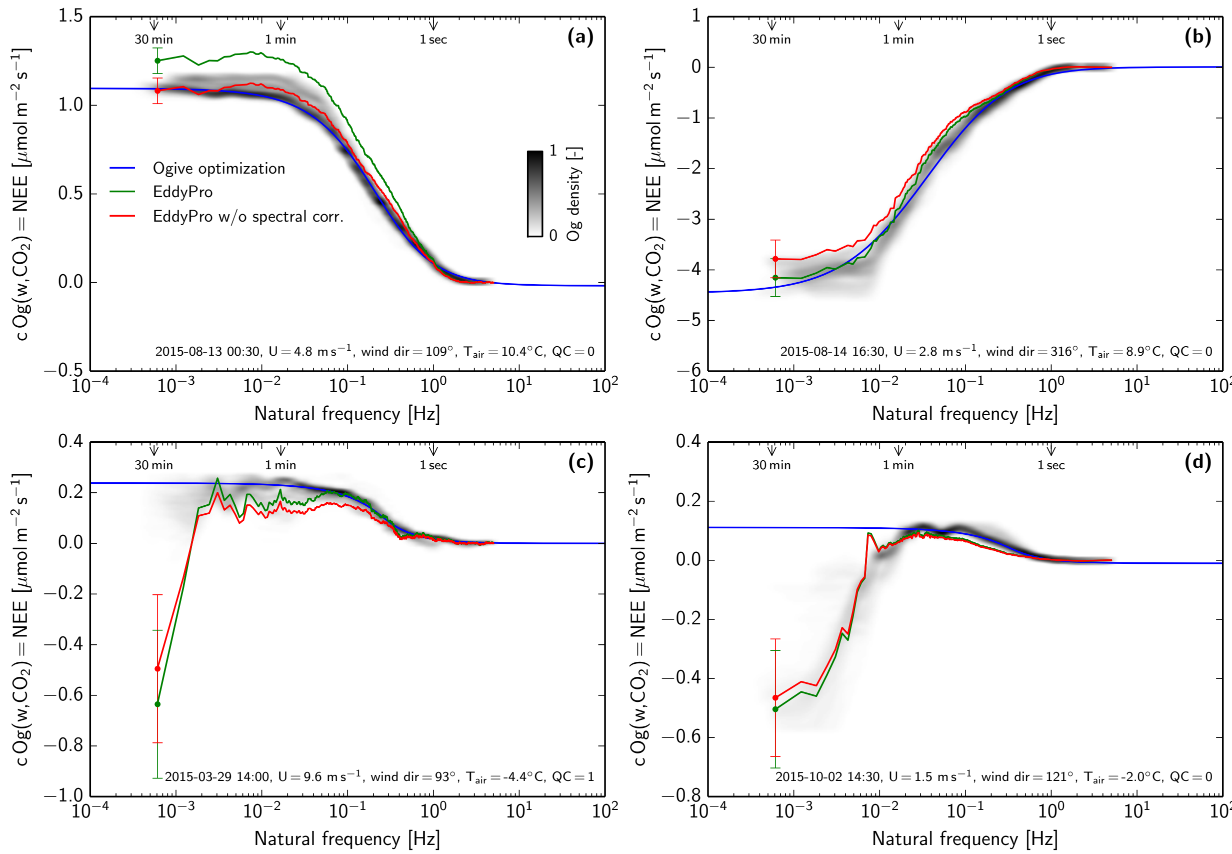

Figure S1: Additional examples of the flux estimation by ogive optimization and EddyPro (with and without spectral corrections after *Moncrieff et al.* (1997, 2004)). Local time, average horizontal wind speed (U), wind direction, air temperature (T_{air}), and quality flag (QC) are given in the lower right of each panel. **(a)** Nighttime release during the growing season showing acceptable agreement between the methods. **(b)** Growing season uptake when both methods agree. **(c)** Small release during strong wind in wintertime. After stabilization of the ogives in the mid-frequency range, contributions of the lowest frequencies implausibly suggest CO_2 uptake in conventional flux estimates. **(d)** Similar situation during calm conditions in October.

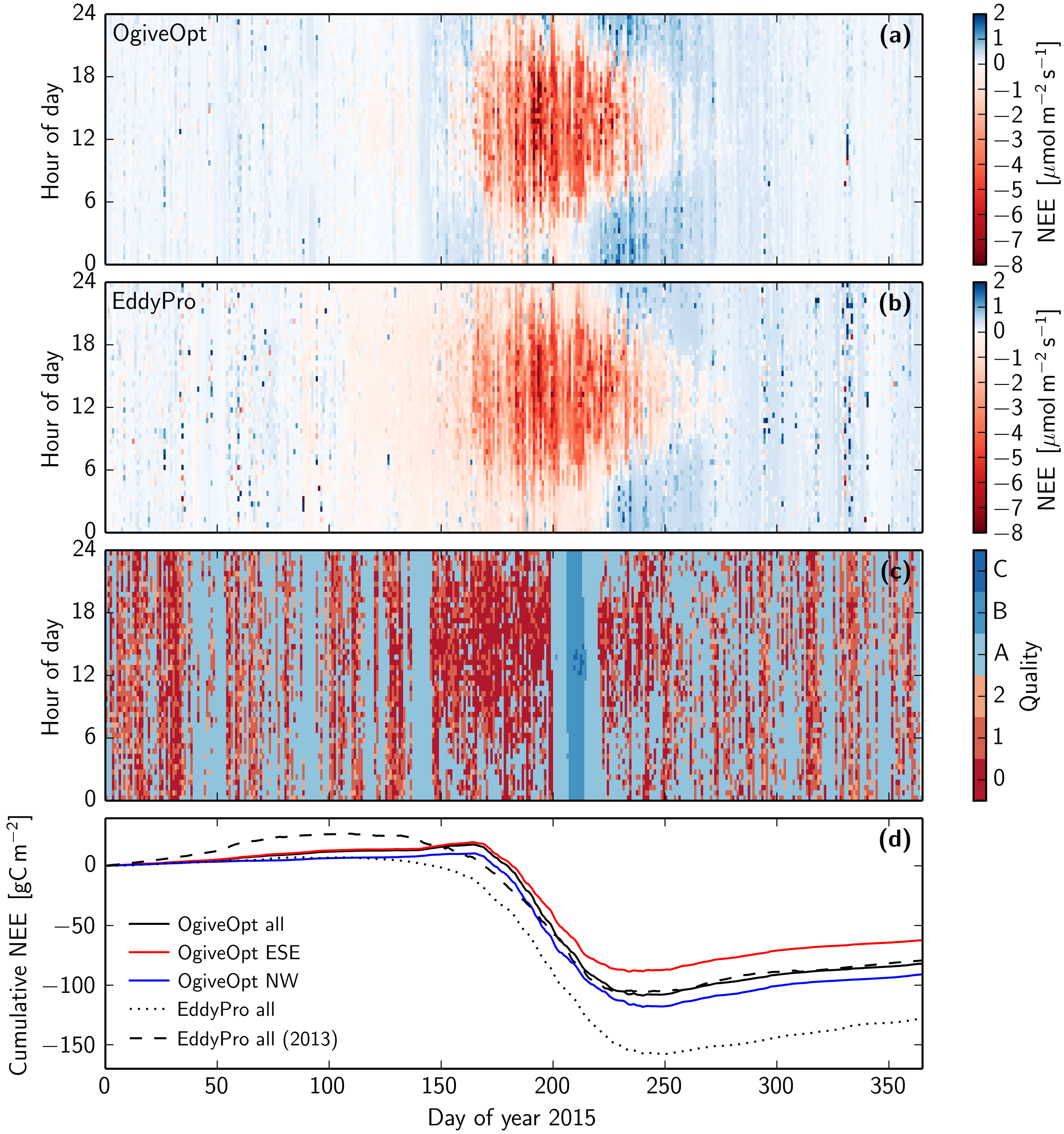

Figure S2: Gap-filled NEE fluxes and quality flags. **(a)** Fingerprint plot of ogive optimization results of 2015. **(b)** Corresponding EddyPro results. **(c)** Corresponding quality flags based on *Foken and Wichura* (1996) and *Reichstein et al.* (2005). **(d)** Cumulative sums based on all measurements, and separately gap filled for the two footprints. The EddyPro results from 2013 are based on raw CO_2 measurements as wet molar densities, which renders them less certain than the 2015 data and prevented flux calculations using ogive optimization.

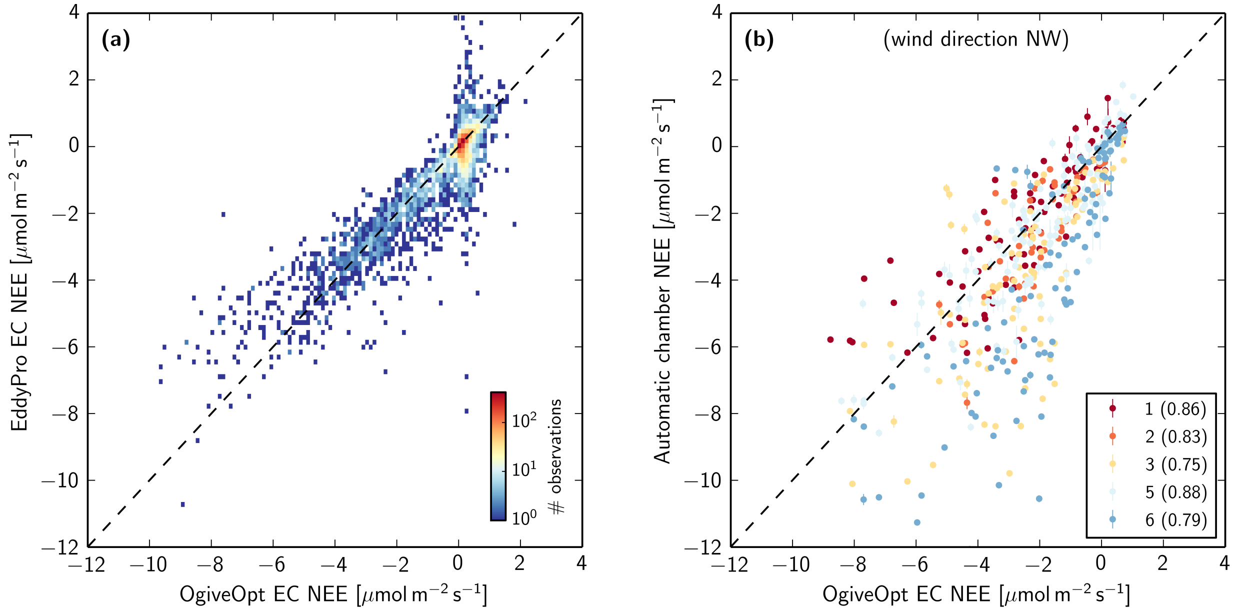

Figure S3: Comparison of ogive optimization fluxes to other methods. **(a)** Histogram of conventional EC fluxes calculated by EddyPro (correlation r=0.88). **(b)** Five individual automatic flux chambers located in the NW footprint (chamber 4 was not operational). Numbers in parentheses denote correlation coefficients. Corresponding p-values are all smaller than 0.0001.

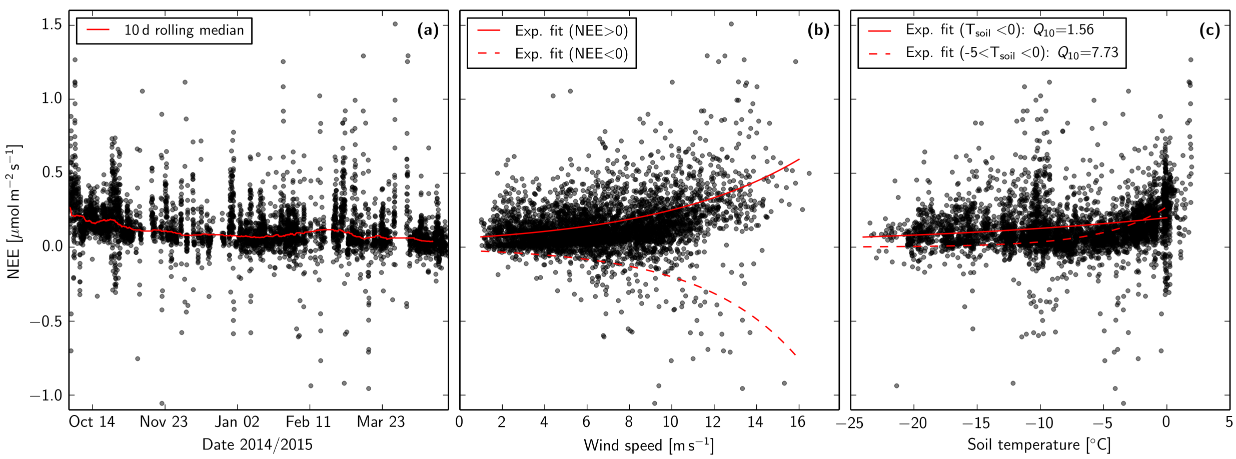

Figure S4: NEE results of ogive optimization between 1 October 2014 and 1 May 2015. **(a)** Time series. **(b)** Relation with wind speed. **(c)** Relation with soil temperature (10 cm depth).

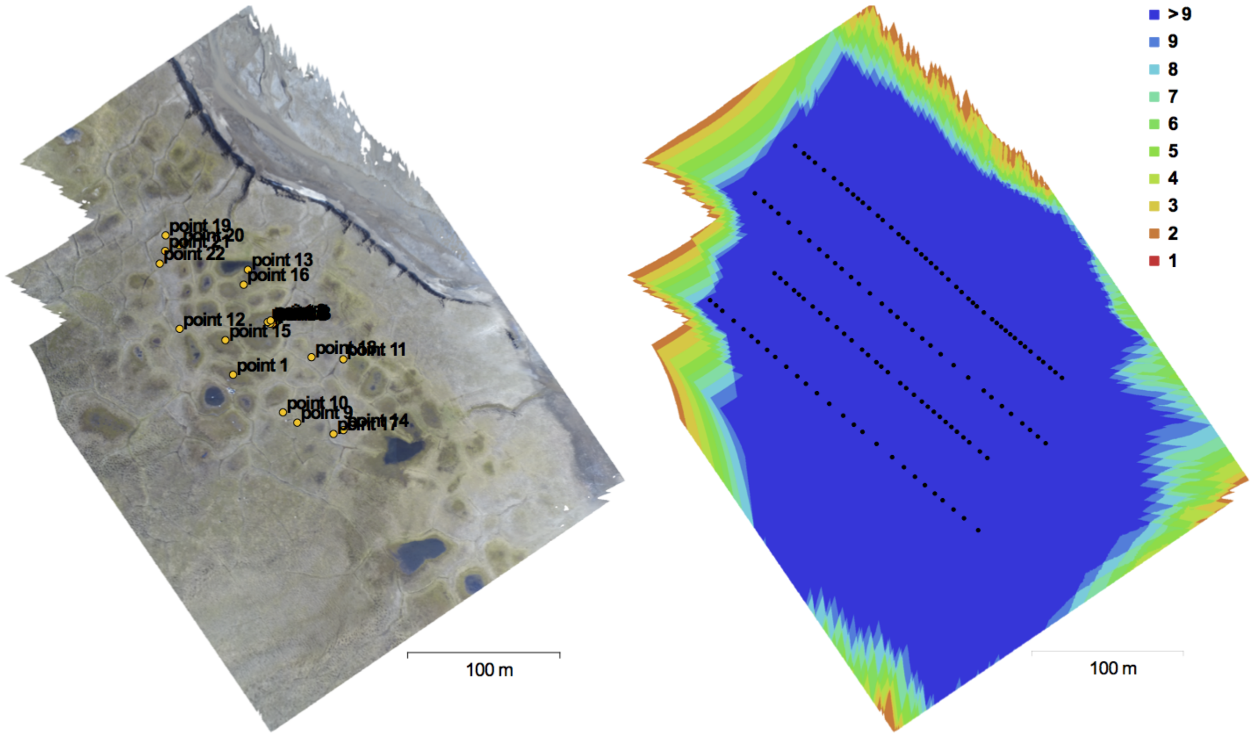

Figure S5: Details of the topographical survey. Left: Ground control points. Right: Camera locations and image overlap.

Figure S6: Photos of the environment and instrumentation on 19 August 2013 (left) and 7 October 2015 (right).

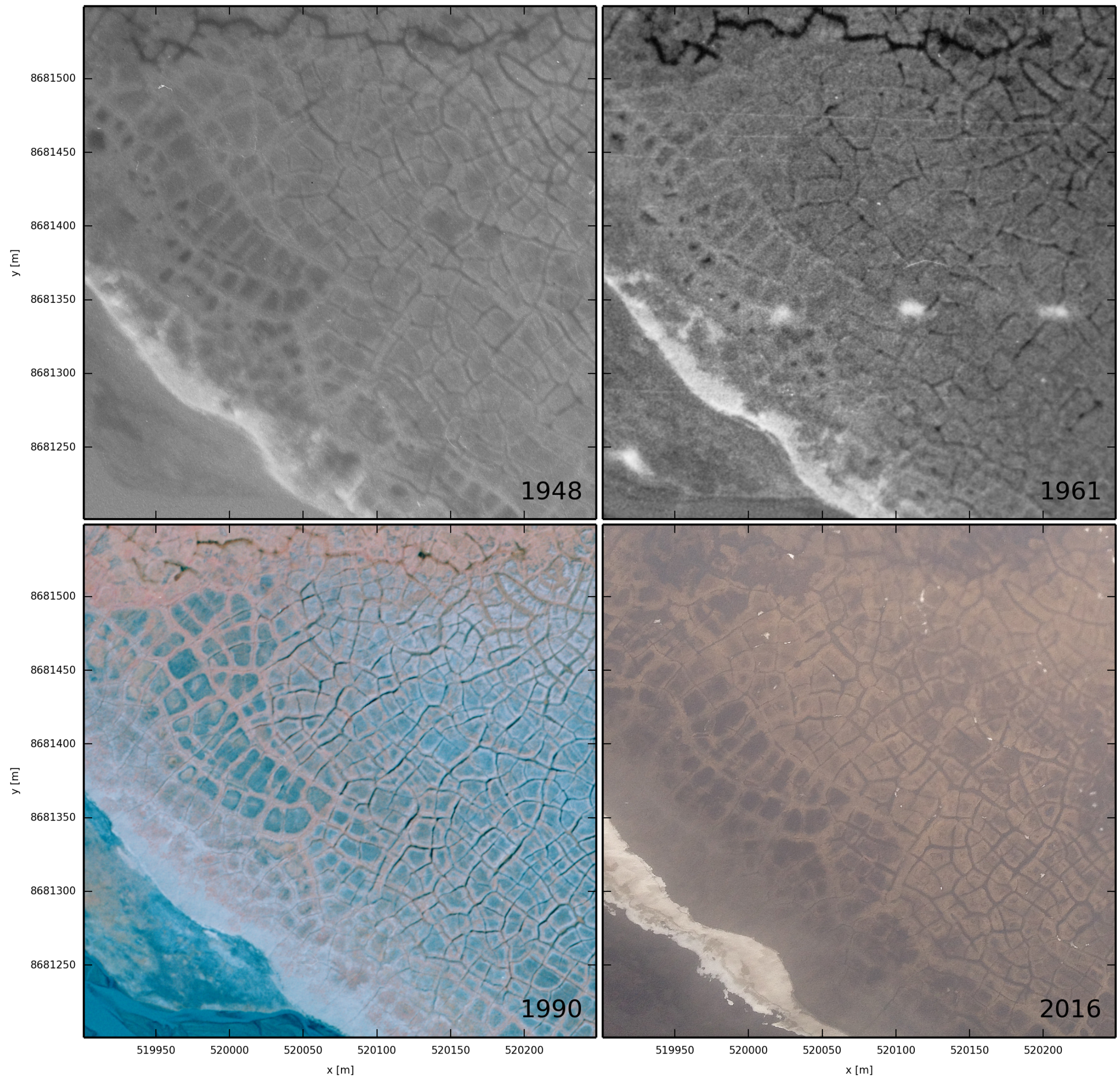

Figure S7: Time series of aerial images from the northern side of Adventdalen, 2.4 km away from the measurement site. Both low-centered and high-centered polygons show little sign of differential ground subsidence, which would indicate ice-wedge degradation. Historical photographs were provided by the Norwegian Polar Institute (reference numbers S48-5181, S61-3301 and S90-5273). The images from 1948 and 1961 were taken on panchromatic film, and the image from 1990 is a near-infrared (false color) photograph.

References

Foken, T., and B. Wichura (1996), Tools for quality assessment of surface-based flux measurements, *Agricultural and forest meteorology*, *78*(1), 83–105.

Moncrieff, J., R. Clement, J. Finnigan, and T. Meyers (2004), Averaging, detrending, and filtering of eddy covariance time series, in *Handbook of micrometeorology*, pp. 7–31, Springer.

Moncrieff, J. B., et al. (1997), A system to measure surface fluxes of momentum, sensible heat, water vapour and carbon dioxide, *Journal of Hydrology*, *188*, 589–611.

Reichstein, M., et al. (2005), On the separation of net ecosystem exchange into assimilation and ecosystem respiration: review and improved algorithm, *Global Change Biology*, *11*(9), 1424–1439.